International Journal of Nanoelectronics and Materials

In Press, Accepted Manuscript – Note to users

Annealing Effects on Band Tail Width, Urbach Energy and Optical Parameters of Fe_2O_3:Ni Thin Films Prepared by Chemical Spray Pyrolysis Technique

N. N. Jandow[1]*, N. F. Habubi[2], S. S. chiad[1], I. A. Al-Baidhany[1], M. A. Qaeed[3]

1. Department of Physics/ College of Education/ Mustansiriyah University/Baghdad- Iraq.
2. Ibn Sina University of Medical of Pharmaceutical Science/ Medical College.
3. Physics Department / Faculty of Science, Jeddah University/Saudi Arabia, Jeddah.

Corresponding author email: nidhaljandow@uomustansiriyah.edu.iq

Abstract

In this research, nickel doped Iron oxide (Fe_2O_3:Ni) thin films were deposited onto glass substrates by using chemical spray pyrolysis (CSP) technique. The deposited films thickness was found to be about 350±30 nm. The films were annealed at two different temperatures (450 and 500^{o}C). The XRD results indicate that the structure of the three prepared thin films was polycrystalline in nature and has a hexagonal phase with preferred orientation along (104) plane. Temperature annealing effects on the optical properties of the deposited films was studied. It was found that, the optical parameters, such as the refractive index (n), the real (ε_1) and imaginary (ε_2) parts of dielectric constant which related to n, Urbach energy and the energy gap depended all on the annealing temperature. The results showed that there was a reduction in the optical absorbance as well as the dielectric constants and the dispersion parameters decreased with increasing the annealing temperature while the determined Urbach energy was increased and the optical energy gap decreased from 2.74 to 2.67 eV with increasing the annealing temperature , on account of there is an inverse relation between Urbach energy and energy gap..

Keywords:

Fe_2O_3:Ni, Structural properties; Optical properties; Dispersion parameters; Urbach energy; Chemical Spray Pyrolysis

1.Introduction

Hematite (α-Fe_2O_3) is a material with a band gap of about 2-2.2eV, this band gap allows absorption ~40% of solar energy via its visible area. Due to this factor Fe_2O_3 is considered to be a promising material for this application. Fe_2O_3 also is low in cost due to abundance in the nature and it is also behave as corrosion-resistant in acidic and alkaline media [1]. This metal oxide has found its way for many other applications according to its dielectric properties and its breakthrough having at once high thermopower [2-7].

However, some major efforts have been done in the fabrication of a Fe_2O_3 photoanode as well as electrocatalyst, such as low electrical conductivity of the material itself and necessity of less than 5 nm particle synthesis, to prevent electron-hole recombination related to the extremely short diffusion distance of holes, among others [8]. By impurity doping, its resistivity can be lowered and considerations of the diffusion length of minority carriers have indicated that p-type Fe_2O_3 could be a better photoanode [9]. Many researchers have been using different techniques for depositing Fe_2O_3 such as; colloidal chemistry method [10], sol-gel [11], usual ceramic technique [12], spray pyrolytic method [13-14], spin coating solution deposition [15], sputtering [16], pulsed laser deposition [17], and molecular beam epitaxy [18] different physical parameters have been studied for this metal oxide material such as the optical and structural parametars.

From the literature, and to our best knowledge, there is no study about the effects of annealing temperature on the optical parameters such as the dispersion parameters and Urbach energy of Fe_2O_3:Ni thin films which prepared utilizing the chemical spray pyrolysis (CSP) technique. In this work, we investigate the effects of annealing temperatures (400, and 500 ºC) on the optical parameters of the deposited Fe_2O_3:Ni thin films by using the chemical spray pyrolysis (CSP) technique.

2. Reserch Methodology

Ni-doped Fe_2O_3 thin films have been prepared by CSP technique. A home made glass atomizer was used for spraying the solution,. The films were deposited onto cleaned glass slides substrates heated to 400 °C. The initial solution was including a o.1 M of $FeCl_3$ (Somatco Supplies Chemicals, India) and 0.1M of $NiCl_2$ (Spectrum Chemicals, India) diluted with redistilled water to obtain an aqueous solution. Few drops of HCl were added in order to obtain a clear solution during the deposition. The volumetric concentration of Ni content was 3%. The optimum conditions was arrived at the following: spraying rate was about 4 ml/min, spraying time was 7 s lasted by (1.5min) to avoid any excessive cooling, the air carrier gas (at a pressure of 10^5 Pascals), and the distance between the nozzle and the substrate was about 28 cm ±1 cm.
Film thickness was measured by gravemetric method and it was found that the thickness was in the range of 350±30 nm. The prepared films were annealed at different temperatures (450 and 500ºC). The optical transmittance and absorbance spectra were recorded in the wavelength range of (380-900nm) by using double beam UV-Visible spectrophotometer (Shimadzu UV probe 1650, Japan).
The average crystallite size (D) of the hematite films was determined by using Scherrer formula[19].

$$D = \frac{K\lambda}{B\cos\theta} \qquad (1)$$

where B is the FWHM (in radians) of XRD intensity, λ is the X-ray wavelength (Cu Kα =0.154 nm), θ is the Bragg diffraction angle, and K is the shape factor which is taken as 0.9.

To determine the total defects in the films, the dislocation density (δ) was calculated using the relation [19]:

$$\delta = \frac{1}{D^2} \qquad (2)$$

The micro strain **(ε)** of the deposited film on the substrate was calculated using the relation [19]:

$$\varepsilon = \frac{\beta\cos\theta}{4} \qquad (3)$$

The real (ε_1) and imaginary (ε_2) parts of dielectric constant are related to the refractive index (n) and extinction coefficient (K) values. The ε_1 and ε_2 values were calculated using the formulas [20]:

$$\varepsilon_1 = n^2 - K^2 \qquad (4)$$

$$\varepsilon_2 = 2nK \quad (5)$$

The amplitude of the electromagnetic wave reduced by a factor of e after passing through a known thickness is called a skin depth (x) which can be calculated by the following relation [21]:

$$x = \frac{\lambda}{2\pi k} \quad (6)$$

In the exponential edge region, Urbach rule is expressed as [22]:

$$A = \alpha_o \exp(h\upsilon/E_U) \quad (7)$$

where α_o is a constant, E_U is the Urbach energy, which characterizes the slope of the exponential edge, and $h\upsilon$ is the photon energy

In order to estimate the refractive index dispersion of the films, the single-oscillator model, developed by DiDomenico and Wemple [23] was used. In terms of the dispersion energy E_d and single-oscillator energy E_o. The single-oscillator model for the refractive index, dispersion is expressed as follows [23]:

$$n^2 - 1 = \frac{E_o E_d}{E_o^2 - E^2} \quad (8)$$

Where E_d and E_o are single oscillator parameters, E_o is the single oscillator energy, E_d is the so-called dispersion energy, which measures the average strength of interband optical transitions, and E is the photon energy ($h\upsilon$).

The oscillator energy E_o is an average of the optical band gap (E_g) [24] and can be obtained by an empirical formula to the optical band gap value: $E_o=2E_g$ [25].

The static refractive index n(0) was evaluated from the equation ($n(0) = 1+E_d/E_o$) and the value of the static dielectric constant ($\varepsilon_\infty = n^2(0)$) was calculated.

The dispersion data of refractive index can be estimated according to the following relation[26]

$$n^2 - 1 = \frac{S_o \lambda_o^2}{1-(\lambda_o/\lambda)^2} \quad (9)$$

Thus the determination of the moments (M_{-1} and M_{-3}) of the ε_i spectrum is very important for the optical applications. M_{-1} and M_{-3} can be obtained from the following relations [27]

$$E_o^2 = \frac{M_{-1}}{M_{-3}} \quad (10)$$

$$E_d^2 = \frac{M_{-1}^3}{M_{-3}} \quad (11)$$

1. Results and Discussions

Figure 1 shows three XRD diffraction patterns of the deposited Fe_2O_3: Ni thin films on glass substrates before and after annealing with 450 ^{O}C and 500 ^{O}C with 2θ peak referred to (012), (104), (110) and (116) direction respectively as compared to the International Center

for Diffraction Data (ICDD), it is clear that the preferred orientation for the three films is in the (104) direction, which means that the films has a hexagonal phase. These results were in good agreement with the results reported by Ubale and Belkhedkar [19].

The figure shows that for the three deposited films; the strong peak value corresponds to (104) direction located at 2θ=33.175, 33.225 and 33.275 with full width at half maximum intensity (FWHM) of 0.45, 0.30 and 0.25 respectively, while the (012, 110 and 116) peaks values are lower intensity than the (104) peak. The figure also shows that as the annealing temperature increases, the diffraction peaks become sharper and their intensity is enhanced; while the FWHM decreases, this indicates that the film structure improved as the annealing temperature increased.

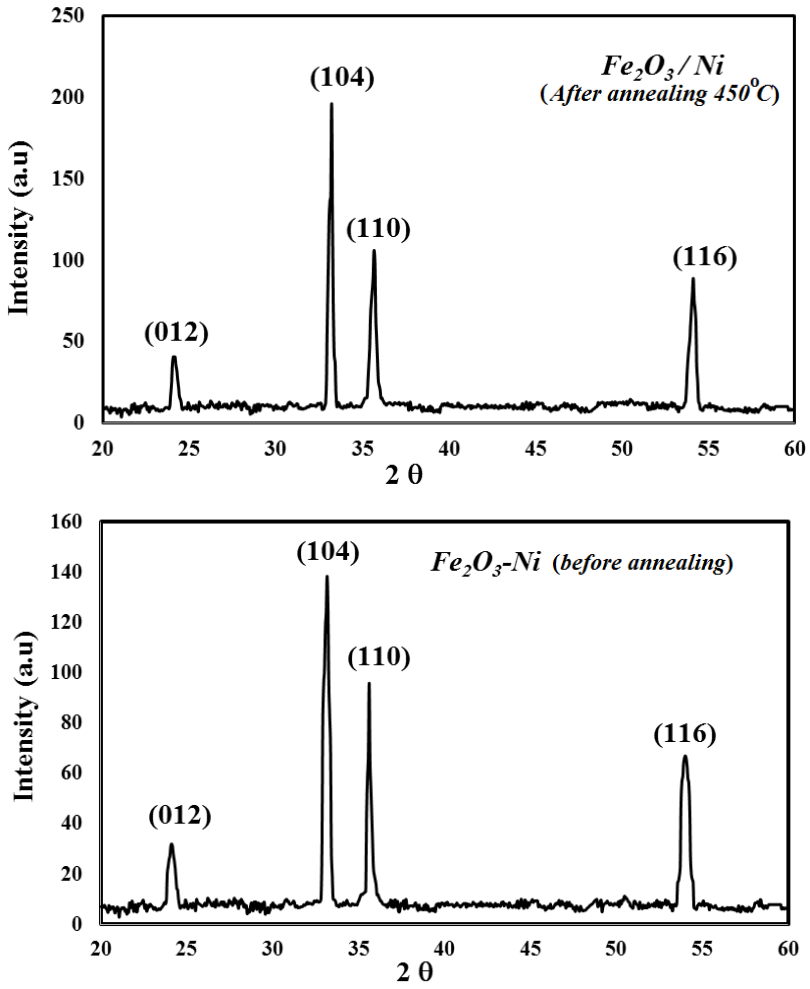

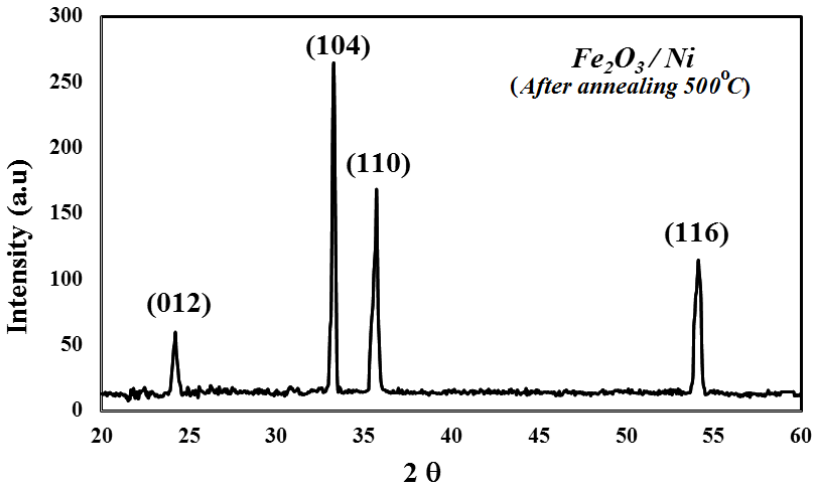

Fig: 1. XRD patterns of Fe_2O_3:Ni thin films before and after annealing at 450 and 500°C.

From the prominent peak (104) by using Scherrer formula (Eq.1), its value was found to be increased as the annealing temperature increases, which indicating that the crystalline quality of the film is improved.

It is found that for the smaller crystallite size the dislocation density is higher and it decreases as crystallite size increases. It is very natural that, when the crystallite size increases and the grain boundaries density decreases; this means that the crystallinity of the thin films is improved.

The micro strain provides the information about the defects present around the lattice. The variation of crystallite size, dislocation density and micro strain values for Fe_2O_3:Ni films deposited before and after annealing at 450 and 500°C are listed in Table 1.

Table 1: X-ray diffraction data summary for the preferential orientation (104) direction for Fe_2O_3:Ni thin films before and after annealing at 450 and 500°C.

Fe_2O_3/Ni	**2θ (°)**	**Peak intensity**	**FWHM (°)**	**Crystallite Size (nm)**	**Dislocation density (δ) (10^{-4} nm^{-1})**	**Micro Strain (ε)×10^{-2}**
Before annealing	33.175	138.513	0.450	18.225	30.106	10.780
Annealing (450°C)	33.225	198.273	0.300	27.340	13.378	7.186
Annealing (500°C)	33.275	264.712	0.250	32.811	0.928	5.988

The absorption spectra of the three deposited Fe_2O_3:Ni thin films before and after annealing with 450 and 500°C respectively are shown in figure 2. From the figure, it can be seen that the absorbance decreases with wavelength and has relatively low values in the

visible (after 550 nm) and IR regions of the spectrum. The results show that the absorbance increases as the annealing tempreture increases. The figure also shows that there is a very small amount optical absorption in the visible region compared to the UV region, hence the film has a potential application in the fabrication of solar cell and UV photodetector.

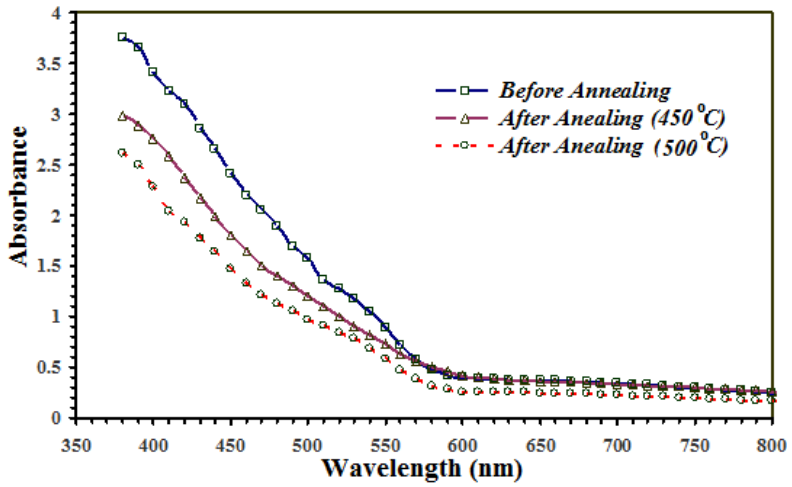

Fig.2: Absorbance spectra of Fe_2O_3:Ni thin films before and after annealing at 450 and 500°C.

The ε_1 and ε_2 values, dependence of wavelength are respectively shown in figures 3 and 4. From the two figures one can see that the ε_1 values are higher than that of ε_2 values and the ε_1 and ε_2 values decrease with increasing of annealing temperatures , the decrease in refractive index could be attributed to the increase of homogeneity of Fe_2O_3: Ni films with anneling temperature.

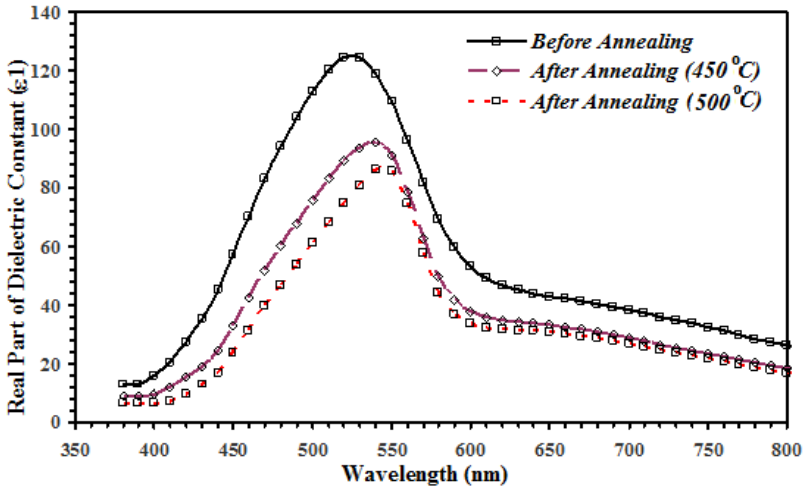

Fig. 3: Plot of the real part of the dielectric constant for Fe_2O_3:Ni thin films before and after annealing at 450 and 500°C.

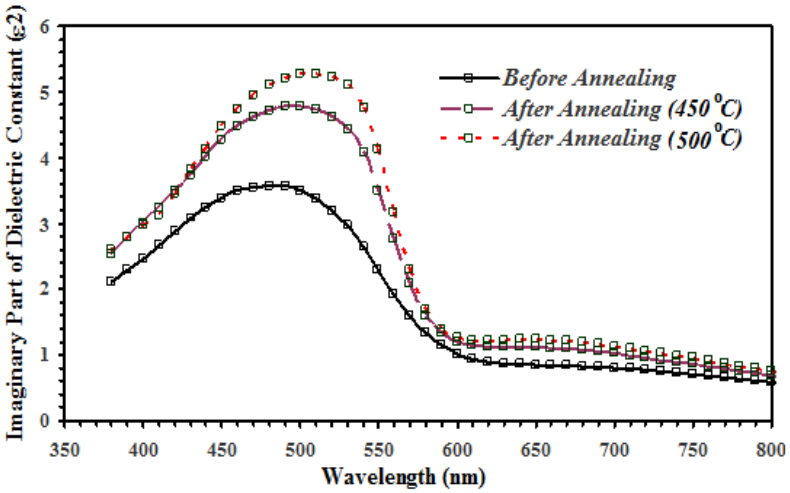

Fig. 4: Plot of the imaginary part of the dielectric constant for Fe_2O_3:Ni thin films before and after annealing at 450 and 500°C.

The skin depth can take the value of one hundred to several thousands of angstrom depending on the kind of the material. Figure 5 shows the variation of skin depth versus wavelength. It can be seen that; at shorter wavelengths there is no change in their values before and after annealing. This might due to the absorption of equal probability in this region, but after λ *(cut off)* (~520nm) the skin depth values became larger as the temperature annealing increases.

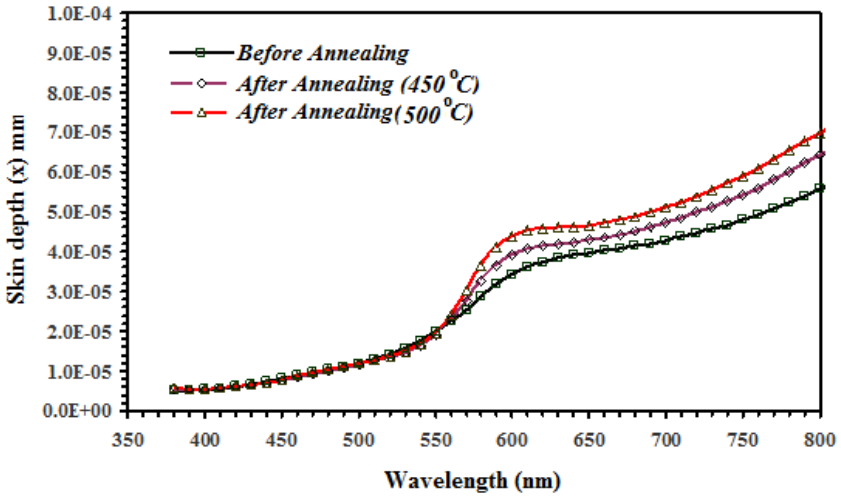

Fig. 5: Plot of skin depth for Fe_2O_3:Ni thin films before and after annealing at 450 and 500°C.

Eq. (7) describes the optical transition between occupied states in the valence band tail to unoccupied states of the conduction band edge. The value of E_U was obtained from the reciprocal of the slope of lnα vs. hν as shown in figure 6 and listed in Table 2.It can be seen that there is an inverse relation between energy gap and Urbach energy , the decrease in the optical enegy gap is attributed to the increase of disorder of the material due to doping[28].

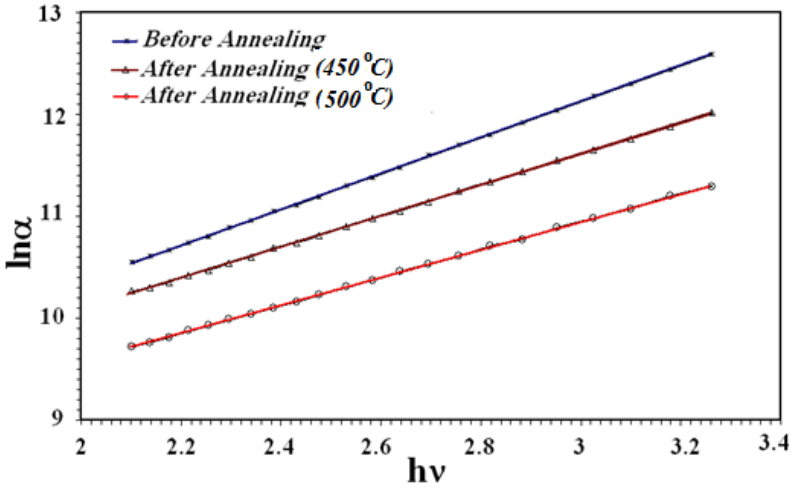

Fig. 6: Ln (α) vs (hυ) for Fe_2O_3:Ni thin films before and after annealing at 450 and 500°C.

From Eq. 8 and by plotting $(n^2-1)^{-1}$ vs. $(h\upsilon)^2$ as illustrated in figure 7; E_o and E_d values were determined from the slope $(E_oE_d)^{-1}$and intercept (E_o/E_d) on the vertical axis respectively. and their values were calculated from the plot of $(n^2-1)^{-1}$vs. $(1/\lambda^2)$ as shown in figure 8. Table 2 summarizes the values of E_o, E_d, n(0), and ε_∞ , So and λ_o for the as-deposited and annealed Fe_2O_3:Ni thin films.

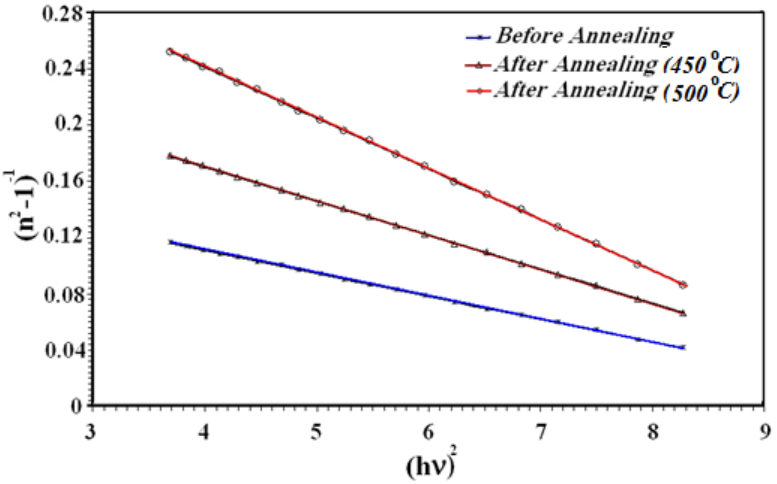

Fig. 7: $(n^2-1)^{-1}$ versus $(h\upsilon)^2$ for Fe_2O_3:Ni thin films before and after annealing at 450 and 500°C.

The single-oscillator parameters E_o and E_d is related to the imaginary of ε_i of the complex dielectric constant. The ε_i parameter includes the desired response information about electronic and optical properties of the used material. , it was found that their values decrease as the annealing temperature increases as shown in Table 2. .This might be due to the dependence of these moment on the complex dielectric constant[29].

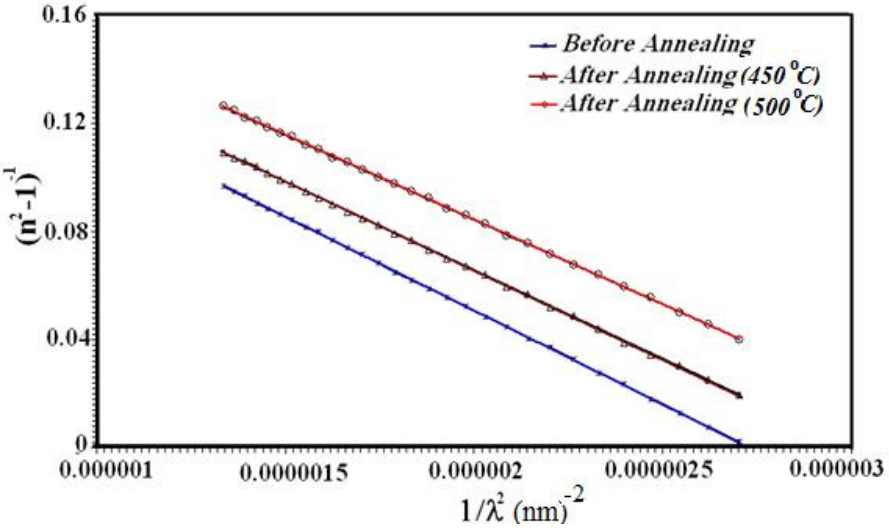

Fig.8: $(n^2-1)^{-1}$ versus $(1/\lambda^2)$ for Fe_2O_3:Ni thin films before and after annealing at 450 and 500°C.

Table 2: The optical parameters of Fe_2O_3:Ni thin films for different annealing temperatures.

Sample	E_d (eV)	E_o (eV)	E_g (eV)	ε_∞	n(o)	M_{-1}	M_{-3} (eV^{-2})	$S_o x10^{13}$ (m^{-2})	λ_o (nm)	U_E (meV)
Before annealing	43.8	5.70	2.85	8.69	2.94	7.69	0.236	2.89	588	451
After annealing (450 °C)	30.0	5.48	2.74	6.55	2.56	5.55	0.185	3.08	519	523
After annealing (500 °C)	20.5	5.34	2.67	4.84	2.20	3.84	0.134	3.20	472	595

2. Conclusion

Fe_2O_3:Ni thin films have been deposited by spray pyrolysis technique on glass substrate with 3% doping of Ni. XRD pattern reveals that all the deposited films were polycrystalline with a preferred orientation along (104) plane. It was found that the optical absorbance decreased as well as the dielectric constants and dispersion parameters such as E_d, E_o, ε_∞, n(0) , λ_o, M_{-1}, and M_{-3} decreased with increasing annealing temperature in contrary

with the values of S_o. The determined Urbach energy increased and the energy gap decreased from 2.74 to 2.67 eV with the increasing of annealing temperature.

Declaration/Acknowledgement

This research did not receive any specific grant from funding agencies in the public, commercial, or not-for-profit sectors.

References

[1] I.A. Raid, Y. Najim, M. Ouda, Spray Pyrolysis Deposition of α Fe_2O_3 Thin Film, e-J. Surf. Sci. Nanotech. 6 (2008) 96-98.
[2] D.G. Wang, C.Z. Chen , J. Ma, T.H. Liu Lead-based titanate ferroelectric thin films fabricated by a sol-gel technique, App. Surf. Sci. 255 (2008) 1637-1645.
[3] D. Biprodas, F.A. Niveen, P.L. Ian, Effect of mixed transition-metal ions in glasses. I. The P_2O_5–V_2O_5–Fe_2O_3 system, J. Non-Cryst. Solids. 351(24-26) (2005) 1958-1966.
[4] N.F. Habubi, K.A. Mishjil, H.G. Rashid, Theortical estimation of direct transitions of Fe [subíndice 2] O [subíndice 3] thin film, Atti. Dell. Fond Gior. Ron. 66(6) (2011) 883-891.
[5] N.J. Mohmmed, N.F. Habubi, Structural and Optical Properties of Fe_2O_3-NiO mixed Thin Films Prepared by Chemical Spray Pyrolysis, Int. lett. Chem. Phys. astron. 14(1) (2014) 65-85.
[6] T.Bak, J. Nowotny, M. Rekas, C.C. SorrellInt, Review: Photo-electrochemical hydrogen generation from water using solar energy. Materials-related aspects, J. Hydrogen Energ. 27 (2002) 991-1022.
[7] A. L.Stroyuk, I. V. Sobran, S.Y. Kuchmiy, Photoinitiation of acrylamide polymerization by Fe_2O_3 nanoparticles, J. Photoch. Photobio. A. 192(2-3) (2007) 98-104.
[8] S. Kuang, L.Yang, S. Luo, Q. Cai, Fabrication, characterization and photoelectrochemical properties of Fe_2O_3 modified TiO_2 nanotube arrays, Appl. Surf. Sci. 255 (16) (2009)7385-7388.
[9] C.C. Leygraf, M. Hendewek, A. G. Somarjoi, The Preparation and Selected Properties of Mg-Doped p-Type Iron Oxide as a Photocathode for the Photoelectrolysis of Water Using Visible Light, J. Solid State Chem. 48 (1983) 357-367.
[10] S.Musić, S. Popović, S. Dalipi, Formation of oxide phases in the system Fe_2O_3 NiO, J. Mater. Sci. 28(7) (1993)1793-1798.
[11] S. Solinas, G. Piccaluga, M. P. Morales, C. J. Serna, Sol-gel formation of γ Fe_2O_3/SiO_2 nanocomposites, Acta mater. 49 (2001) 2805-2811.
[12] S. Mohanty and J. Ghose, Studies on Some α-Fe_2O_3 Photoelectrodes, J. Phys. Chem. Solids. 53(1) (1992) 81-91.
[13] N.Khademi, M.M.Bagheri-Mohagheghi, The Structural, Thermoelectric and Optical Properties of SnO_2-Fe_2O_3: Bi Thin Films Deposited by Spray Prolysis Technique, T.E.P.E. 2(3) (2013) 89-93.
[14] J.D. Desai, H.M.Pathan, S.K.Min, K.D. Jung, O.S. Joo, Preparation and Characterization of Iron Oxide Thin Films by Spray Pyrolysis using Methanolic and Ethanolic Solutions, App. Surf. Sci. 252 (2006)2251-2258.

[15] F. L.Souza, K. P.Lopes, E. Longo, E. R. Leite, The influence of the film thickness of nanostructured alpha-Fe_2O_3 on water photooxidation, Phys. Chem. Phys. 11 (2009) 1215-1219.
[16] J. Chavez-Galan, R. Almanza, Solar filters based on iron oxides for energy savings with efficient windows, Sol. Energ. 81(1) (2007) 13-19.
[17] M. G. Chapline and S.X. Wang, Observation of the Verwey transition in thin magnetite films, J. Appl. Phys. 97(12) (2005)123901-3.
[18] S. k. Arora, G. R. S. Sumesh, I. Shvets, M. Luysberg, Anomalous strain relaxation behavior of Fe_3O_4/MgO (100) heteroepitaxial system grown using molecular beam epitaxy, J. Appl. Phys. 100 (2006) 3908-073908.
[19] A. U. Ubale and M. R. Belkhedkar, Size Dependent Physical Properties of Nanostructured α-Fe_2O_3 Thin Films Grown by Successive Ionic Layer Adsorption and Reaction Method for Antibacterial Application, J. Mater. Sci. Technol. 31(1) (2015)1-9.
[20] S. Moss, J. G. Burrell, B. Ellis, Semiconductor Opto-Electronics, Wiley, New York,1973.
[21] J. F. Eloy, Power Lasers, National School of Physics, Grenoble, France, John Wiley & Sons,1984.
[22] J. Tauc, Amorphous and Liquid Semiconductors, Plenum Press, New York, 1974.
[23] M. DiDomenico, and S. H. Wemple, Oxygen-Octahedra Ferroelectrics. I. Theory of Electro-Optical and Nonlinear-Optical Effects, J. Appl. Phys. 40 (1969) 720-734.
[24] H. S. Wemple and M. Didomenico, Behavior of the Electronic Dielectric Constant in Covalent and Ionic Materials, Phys. Rev. B. 3 (1971)1338-1351.
[25] M.Modreanu, M.Gartner, N.Tomozeiu, , J. Seekamp, P. Cosmin, Investigation on optical and microstructural properties of photoluminescent LPCVD SiO_xN_y thin films, Opt. Mater. 17 (2001)145-148.
[26] A. F. Quasrawi and M.M S.. Ahmad, Optoelectronical properties of polycrystalline β-GaSe thin films, Cryst. Res. Technol. 41(2006) 364-370.
[27] S. H. Wemple and M. DiDomenico, Optical Dispersion and the Structure of Solids, Phys. Rev. Lett. 23 (1969)1156-1160.
[28] Saliha Ilican,Yasemin Caglar,Mujdat Caglar, Faherettin Yakuphanoglu,Structural ,optical and electrical properties of F-doped ZnO nanrod semiconductor thin films deposited by dol-gel process,Applied Surface Science 255(2008)2353-2359.
[29] Mujdat Caglar,Saliha Ilican,Yasemin Caglar,Structural mmorphological and optical properties of $CuAlS_2$ films deposited by spray pyrolysis method, Optics Communications 281(2008) 1615-1624.